

# NODESIG: Random Walk Diffusion meets Hashing for Scalable Graph Embeddings

Abdulkadir Çelikkanat  
Paris-Saclay University  
CentraleSupélec, Inria  
France

abdulkadir.celikkanat@centralesupelec.fr

Apostolos N. Papadopoulos  
Aristotle University of Thessaloniki  
Department of Informatics  
Greece

papadopo@csd.auth.gr

Fragkiskos D. Malliaros  
Paris-Saclay University  
CentraleSupélec, Inria  
France

fragkiskos.malliaros@centralesupelec.fr

## ABSTRACT

Learning node representations is a crucial task with a plethora of interdisciplinary applications. Nevertheless, as the size of the networks increases, most widely used models face computational challenges to scale to large networks. While there is a recent effort towards designing algorithms that solely deal with scalability issues, most of them behave poorly in terms of accuracy on downstream tasks. In this paper, we aim at studying models that balance the trade-off between efficiency and accuracy. In particular, we propose NODESIG, a scalable embedding model that computes binary node representations. NODESIG exploits random walk diffusion probabilities via stable random projection hashing, towards efficiently computing embeddings in the Hamming space. Our extensive experimental evaluation on various graphs has demonstrated that the proposed model achieves a good balance between accuracy and efficiency compared to well-known baseline models on two downstream tasks.

## CCS CONCEPTS

• **Information systems** → **Data mining; Social networks.**

## KEYWORDS

graph mining, network representation learning, node embeddings, node classification, link prediction

## 1 INTRODUCTION

Graph-structured data is ubiquitous in many diverse disciplines and application domains, including information, biology, and networks arising from social media and networking platforms [16]. Besides being elegant models for data representation, graphs have also been proven valuable in various widely used machine learning tasks. For instance, in the case of biological networks, we are interested to predict the function of proteins or to infer the missing structure of the underlying protein-protein interaction network. Both of these problems can be formalized as learning tasks on graphs, with the main challenge being how to properly incorporate its structural properties and the proximity among nodes into the learning process. To this direction, *representation learning on graphs* has become a key paradigm for extracting information from networks and for performing various tasks such as link prediction, classification and visualization [9]. These models aim to find a vector representation of the nodes of the graph (i.e., *node embeddings*) in a way that the

desired properties and proximity among nodes are preserved in the embedding space.

Most of the existing node representation learning approaches deal with *learning-based models*, relying either on matrix factorization or on node context sampling to infer the proximities between nodes [9]. For the former, the goal is to learn embeddings by *factorizing* the matrix which has been designed for capturing and representing desired graph properties and node proximities in a lower dimensional space. Typically, such approaches target to preserve first-order (adjacency-based) or higher-order proximity of nodes (e.g., GRAREP [3], SDNE [31], and HOPE [18]), leveraging the Singular Value Decomposition (SVD) to obtain a low-rank approximation of the proximity matrix. Nevertheless, these models face computational challenges since they rely on expensive factorization of dense node proximity matrices—thus, making them prohibited for large networks. Although recent studies have proposed heuristics to reduce the complexity of matrix factorization [6, 38], such models lack flexibility since they still rely on user-specified, hand-designed proximity criteria.

In order to address the aforementioned challenges towards developing effective and scalable algorithms for representation learning on networks, *random walk*-based models have gained considerable attention [9]. The main idea here is to learn node embeddings by maximizing the probability of node co-occurrences in random walk sequences (e.g., DEEPWALK [20], NODE2VEC [8], BIASEDWALK [17] and EFGE [4]). Nevertheless, besides the inherent model optimization cost (e.g., via *Stochastic Gradient Descent*), a large number of random walks is required to be explicitly sampled in order to ensure the effectiveness of the embedding on downstream tasks (e.g., link prediction, node classification). Furthermore, it has been shown that random walk embedding approaches that leverage SKIP-GRAM [15] to model node co-occurrences, implicitly perform factorization of a properly chosen dense transition probability matrix, leading to better performance on downstream tasks [23]. Although recent studies aim to improve running time complexity via matrix sparsification tools [22] or capitalizing on hierarchical graph representations [1, 5], the quality of the embeddings deteriorates significantly.

Besides the computational burden of model optimization, most of the proposed algorithms learn low-dimensional embeddings in the *Euclidean* space. This makes their applicability challenging due to scalability issues of the *cosine* distance computation typically used while examining similarity between embeddings. To address this challenge, recent studies have proposed to learn *discrete* node representations [14, 33, 34], in which *Hamming* distance is leveraged to determine embeddings similarity. The basic idea builds upon fast sketching techniques for scalable similarity search, mainly based

on data-independent or data-dependent hashing techniques [32]. Although binary embeddings speedup distance measure computations, the corresponding models often undergo computationally intensive learning procedures especially in the case of learning-to-hash models [14]. While recent data-independent hashing models have been introduced for node embeddings [34], they lack flexibility on the way that context nodes are chosen. Besides, relying on MINHASH for similarity estimation [2], prohibits the computation of embeddings on dynamic graphs.

**Contributions.** In this paper, we propose NODESIG, a scalable model for computing expressive binary node embeddings based on stable random projections. NODESIG first leverages random walk diffusions to estimate higher-order node proximity. Then, a properly defined sign random projection hashing technique is applied to obtain binary node signatures. Each component of NODESIG has been designed to ensure the scalability of the model, while at the same time the accuracy on downstream tasks is not compromised or even improves compared to traditional models. Fig. 1 positions NODESIG regarding accuracy and running time, providing a comparison to different models on the *DBLP* network. As we can observe, NODESIG’s running time is comparable to the one of models that focus solely on scalability (e.g., NODESKETCH, RANDNE, LOUVAINNE), with improved accuracy even higher than NODE2VEC or HOPE on this particular dataset.

The main contributions of the paper can be summarized as follows:

- We introduce NODESIG, a scalable and expressive model for binary node embeddings based on stable random projection hashing of random walk diffusion probabilities. NODESIG leverages higher-order proximity information among nodes, while its design allows to scale to large graphs without sacrificing accuracy.
- The distance computation between node signatures in the embedded space is provided by the Hamming distance on bit vectors, which is significantly more efficient than distance computations based on other distance measures. Besides, NODESIG can easily be extended to deal with dynamic networks.
- In a thorough experimental evaluation, we demonstrate that the proposed binary embeddings achieve superior performance compared to various baseline models on two downstream tasks. At the same time, the running time required to compute node signatures allow the model to scale on large graphs.

**Roadmap.** The rest of the paper is organized as follows. Section 2 presents related work in the field. Section 3 presents the proposed approach in detail. Performance evaluation results are offered in Section 4, whereas Section 5 summarizes the work and discusses briefly future work in the area.

**Source code.** The implementation of the proposed model in C++ can be found in the following link: <http://tiny.cc/0t2osz>.

## 2 RELATED WORK

Graphs are rich representations of the real world that can capture different types of relationships and modalities among entities. However, representing nodes as vectors is a very promising direction

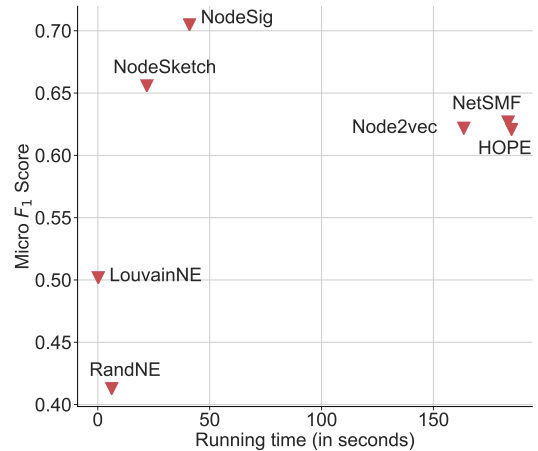


**Figure 1: Comparison of models on *DBLP* network. NODESIG balances between good accuracy and low running time.**

towards fast and accurate knowledge discovery. The literature is rich in algorithmic techniques to map nodes (as well as edges or whole graphs) to low-dimensional vectors [9].

Since the concept of graph embedding is similar to that of dimensionality reduction, techniques like LLE [24], IsoMap [29] or Multi-Dimensional Scaling (MDS) [37] may be used to provide the necessary low-dimensional representations. These techniques take as input a matrix  $n \times m$  and deliver a matrix  $n \times d$ , where  $d \ll m$ , is the dimensionality of the target space. However, the high computational cost of those algorithms motivated researchers to design more scalable techniques.

One of the first modern algorithms was proposed in [20]. The DEEPWALK algorithm uses uniform truncated random walks to represent the *context* of a node. Intuitively, nodes with similar random walks have a higher degree of similarity. A generalization of DEEPWALK was proposed in [8]. The NODE2VEC algorithm is more general and manages to combine BFS and DFS search strategies, achieving significant performance improvements and being able to capture node similarities even in cases where nodes are very close to each other (based on number of hops). Essentially those techniques constitutes adaptations of the SKIPGRAM technique proposed in [15] for word embeddings.

The LINE method, proposed in [26], optimizes an objective function that captures both first-order and second-order proximity of each node. An advantage of LINE is that it can be applied on weighted networks as well. A carefully designed edge sampling technique that is used (negative sampling) avoids the serious performance limitations of stochastic gradient descent and related techniques.

It turns out that problems related to random walk sampling can be alleviated by using matrix factorization. The NETMF technique proposed in [23], essentially generalizes DEEPWALK, NODE2VEC and LINE. The main drawback of NETMF, however, is that in general matrix factorization is a computationally intensive operation.

The main limitation of the aforementioned embedding techniques is that they do not scale well for large networks. The main focus has been put on increasing the effectiveness of data mining

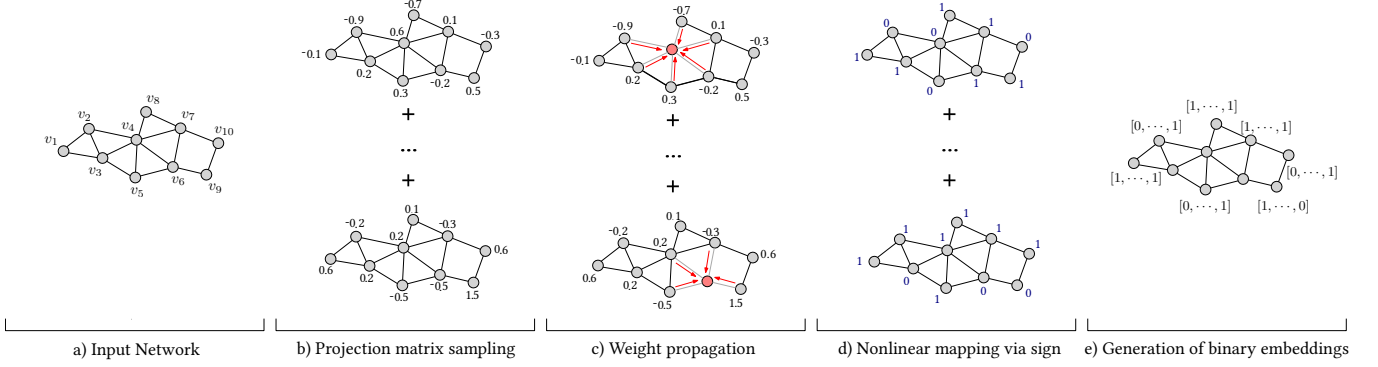


**Figure 2: Schematic representation of the NODESIG model. Firstly, the weights of the random projection matrix are sampled and then the projection of the proximity matrix is performed via the weight propagation step. Finally, binary node representations are obtained by combining the signs of the projected values.**

tasks (e.g., classification, link prediction, network reconstruction) whereas the efficiency dimension has not received significant attention. To attack this problem, recent advances in network representation learning use random projection or hashing techniques (more specifically, variants of locality-sensitive hashing) in order to boost performance, trying to maintain effectiveness as well.

One of the first scalable approaches (RANDNE) was proposed in [38]. RANDNE is based on iterative Gaussian random projection, being able to adapt to any desired proximity level. This results in significantly better performance than techniques based on random walks or matrix factorization. In the same line, FASTRP was proposed in [6] which is faster than RANDNE and also more accurate.

Recently, embedding techniques based on hashing have emerged as a promising alternative to enable faster processing while at the same time retain good accuracy results. The NETHASH algorithm, proposed in [33], expands each node of the graph into a rooted tree, and then by using a bottom-up approach encodes structural information as well as attribute values into minhash signatures in a recursive manner. A similar approach has been used in NODESKETCH [34], where the context of every node is defined in a different way whereas the embedding vector of each node contains integer values and the weighted Jaccard similarity coefficient is being used. Based on performance evaluation results reported in [34], NODESKETCH is extremely efficient managing to reduce the embedding cost by orders of magnitude in comparison to baseline approaches. Moreover, NODESKETCH achieves comparable (or even better) F1 score in the node classification task as well as comparable or better precision in the link prediction task with respect to the baseline techniques.

The NODESIG model proposed in this paper, takes a different approach. First, it samples weights from the Cauchy distribution in order to construct the projection matrix. Then, it obtains the projected values by performing recursive update rules instead of explicitly realizing the data matrix. Finally, a bit-vector is generated, corresponding to the signature of the projected data. As we will demonstrate shortly, NODESIG shows comparable or even better accuracy results compared to NODESKETCH, while at the same time, it can easily be adapted to be applied in more demanding settings like dynamic or streaming environments.

### 3 PROPOSED APPROACH

In this section, we will introduce the proposed approach, referred to as NODESIG, which aims at representing the nodes of the network as fixed-length binary codes. The model mainly relies on sign stable random projections of a properly designed matrix that captures higher order proximity among nodes. Initially, we will describe how we construct this target matrix by using random walk diffusion probabilities, and then we will demonstrate how the random projections can be performed by propagating the sampled weights. Finally, we obtain the binary representations by incorporating a nonlinear mapping through a simple sign function. An overview of the basic steps of NODESIG is given in Figure 2.

Throughout the paper, we will use  $\mathcal{G} = (V, E)$  to denote a graph where  $V := \{v_1, \dots, v_N\}$  is the vertex set and  $E \subset V \times V$  is the edge set. Its adjacency matrix is represented by  $A$  and the notations  $A_{(i,j)}$  or  $A[v_i, v_j]$  are used to indicate the value in the  $i$ th and  $j$ th column. It is also assumed that the networks are undirected.

#### 3.1 Random Walk Diffusion for Node Proximity Estimation

In most cases, direct links among nodes are not sufficient to grasp various inherent properties of the network that are related to node proximity. It is highly probable that the network might have missing or noisy connections, thus relying solely on first-order proximity can reduce the expressiveness of the model. Random walk diffusions constitute an interesting way to leverage higher-order information while computing embeddings. The underlying idea relies on the co-occurrence frequencies of nodes up to a certain distance in the random walks; nodes appearing more frequently close to each other within the random walks, share similar characteristics, and therefore should be placed close to each other in the embedding space. This idea has been exploited by various representation learning models, including DEEPWALK [20] and NODE2VEC [8]. Nevertheless, sampling multiple random walks, as used in various models (e.g., [4, 8, 20]), significantly increases the training time causing scalability issues.

To overcome this problem, in this paper we directly leverage random walk diffusions, adopting a uniform random walking strategy

to extract information describing the structural roles of nodes in the network. Let  $\mathbf{P}$  used to denote the right stochastic matrix associated with the adjacency matrix of the graph, which is obtained by normalizing the rows of the matrix. More formally,  $\mathbf{P}$  can be written as  $P_{i,j} := A_{i,j}/\sum_j A_{i,j}$ , defining the transition probabilities of the uniform random walk strategy. We use a slightly modified version of the transition matrix by adding a self-loop on each node, in case it does not exist.

Note that, the probability of visiting the next node depends only on the current node that the random walk resides; therefore, node  $v_j$  can be visited starting from  $v_i$  and taking  $l$  steps with probability  $P_{i,j}^l$ , if there is a path connecting them. For a given walk length  $L$ , we define the matrix  $\mathbf{M}$  as

$$\mathbf{M} := \mathbf{P} + \dots + \mathbf{P}^l + \dots + \mathbf{P}^L,$$

where  $\mathbf{P}^l$  indicates the  $l$ -order proximity matrix and each entry  $M_{i,j}$  in fact specifies the expectation of visiting  $v_j$  starting from node  $v_i$  in  $l$  steps. By introducing an additional parameter  $\alpha$ ,  $\mathbf{M}(\alpha)$  can be rewritten as follows:

$$\mathbf{M}(\alpha) := \alpha\mathbf{P} + \dots + \alpha^l\mathbf{P}^l + \dots + \alpha^L\mathbf{P}^L.$$

Higher order node proximities can be captured using longer walk lengths, where the impact of the walk at different steps is controlled by the *importance factor*  $\alpha$ . As we will present in the next paragraph, matrix  $\mathbf{M}(\alpha)$  is properly exploited by a random projection hashing strategy to efficiently compute binary node representations.

### 3.2 Learning Binary Embeddings

Random projection methods [30] have been widely used in a wide range of machine learning applications that are dealing with large scale data. They mainly target to represent data points into a lower dimensional space by preserving the similarity in the original space. Here, we aim at encoding each node of the network in a *Hamming* space  $\mathbb{H}(d_{\mathcal{H}}, \{0, 1\}^{\mathcal{D}})$ ; we consider the normalized *Hamming* distance  $d_{\mathcal{H}}$  as the distance metric [36]. The benefit of binary representations is twofold: first, they will allow us to perform efficient distance computation using bitwise operations, and secondly reduce the required disk space to store the data.

Random projections are linear mappings; the binary embeddings though require nonlinear functions to perform the discretization step, and a natural choice is to consider the signs of the values obtained by *Johnson-Lindenstrauss* [12] transform. More formally, it can be written that

$$h_{\mathbf{W}}(\mathbf{x}) := \text{sign}(\mathbf{x}^{\top}\mathbf{W}),$$

where  $\mathbf{W}$  is the projection matrix whose entries  $\mathbf{W}_{(i,j)}$  are independently drawn from normal distribution and  $\text{sign}(\mathbf{x}_i)$  is equal to 1 if  $\mathbf{x}_i > 0$  and 0 otherwise.

The approach was first introduced by Goemans and Williamson [7] for a rounding scheme in approximation algorithms, demonstrating that the probability of obtaining different values for a single bit quantization is proportional to the angle between vectors, as it is shown in Theorem 1. The main idea relies on sampling uniformly distributed random hyperplanes in  $\mathbb{R}^{\mathcal{D}}$ . Each column of the

projection matrix, in fact, defines a hyperplane in  $\mathbb{R}^{\mathcal{D}}$  and the arc between vectors  $\mathbf{x}$  and  $\mathbf{y}$  on the unit sphere is intersected if  $h_{\mathbf{W}}(\mathbf{x})_i$  and  $h_{\mathbf{W}}(\mathbf{y})_i$  takes different value.

**THEOREM 1** ([7]). *For a given pair of vectors  $\mathbf{x}, \mathbf{y} \in \mathbb{R}^N$ ,*

$$\mathbb{P}[h_{\mathbf{W}}(\mathbf{x}) \neq h_{\mathbf{W}}(\mathbf{y})] = \frac{1}{\pi} \cos^{-1} \left( \frac{\mathbf{x} \cdot \mathbf{y}}{\|\mathbf{x}\|_2 \|\mathbf{y}\|_2} \right)$$

where  $w_i \sim \mathcal{N}(0, 1)$  for  $1 \leq i \leq N$ .

The *stable* random projections approach [13] generalizes the aforementioned idea using a symmetric  $\alpha$ -stable distribution with unit scale in order to sample the elements of the projection matrix, for  $0 < \alpha \leq 2$ . Li et al. [13] proposed an upper bound, where

$$\mathbb{P}[h_{\mathbf{W}}(\mathbf{x}) \neq h_{\mathbf{W}}(\mathbf{y})] \leq \frac{1}{\pi} \cos^{-1} \rho_{\alpha}$$

for non-negative vectors ( $\mathbf{x}_i \geq 0, \mathbf{y}_i \geq 0$  for  $1 \leq i \leq N$ ) and  $\rho_{\alpha}$  is defined as

$$\rho_{\alpha} := \left( \frac{\sum_{i=1}^d \mathbf{x}_i^{\alpha/2} \mathbf{y}_i^{\alpha/2}}{\sqrt{\sum_{i=1}^d \mathbf{x}_i^{\alpha}} \sqrt{\sum_{i=1}^d \mathbf{y}_i^{\alpha}}} \right)^{2/\alpha}.$$

It is well known that the bound is exact for  $\alpha = 2$ , which also corresponds to the special case in which normal random projections are performed. When the vectors are chosen from the  $\ell^1(\mathbb{R}^+)$  space (i.e.,  $\sum_{d=1} x_d = 1, \sum_{d=1} y_d = 1$ ), it is clear to see that the  $\chi^2$  similarity  $\rho_{\chi^2}$  defined as  $\sum_{d=1} (2x_d y_d)/(x_d + y_d)$  is always greater or equal to  $\rho_1$ . It has empirically shown [13] that the collision probability for *Cauchy* random projections with unit scale can be well estimated, especially for sparse data:

$$\mathbb{P}[h_{\mathbf{W}}(\mathbf{x}) \neq h_{\mathbf{W}}(\mathbf{y})] \approx \frac{1}{\pi} \cos^{-1} \rho_{\chi^2} \leq \frac{1}{\pi} \cos^{-1} \rho_1.$$

Note that, matrix  $\mathbf{M}(\alpha)$  described in the previous paragraph consists of non-negative values; its row sums are equal to  $\sum_{d=1}^L \alpha^d$  and  $\mathbf{M}(\alpha)$  is sparse enough for small walk lengths. Therefore, we design the projection matrix by sampling its entries from the *Cauchy* distribution, aiming to learn binary representations preserving the *chi-square* similarity. The chi-square distance is one of the measures used for histogram-based data, commonly used in the fields of computer vision and natural language processing [11, 35].

As it is shown in Figure 2, the last step of **NODESIG** for obtaining binary node representations is by using the signs of projected data. In other words, the embedding vector  $E[v_i]$  for each node  $v_i \in V$  is computed as follows:

$$E[v_i] := \left[ \text{sign} \left( \mathbf{M}_{(i,:)}(\alpha) \cdot \mathbf{W}_{(:,1)} \right), \dots, \text{sign} \left( \mathbf{M}_{(i,:)}(\alpha) \cdot \mathbf{W}_{(:,\mathcal{D})} \right) \right].$$

Note that, the projection of the exact realization of  $\mathbf{M}(\alpha)$  can be computationally intensive, especially for large walks. Instead, it can be computed by propagating the weights  $\mathbf{W}_{(u,d)}$  for each dimension  $d$  ( $1 \leq d \leq \mathcal{D}$ ), using the following recursive update rule:

$$\mathcal{R}_{(v,d)}^{l+1}(\alpha) \leftarrow \alpha \sum_{u \in \mathcal{N}(v)} \left( \mathbf{W}_{(u,d)} + \mathcal{R}_{(u,d)}^l(\alpha) \right) \times \mathbf{P}_{(u,v)}, \quad (1)$$

where  $\mathcal{N}(v)$  refers to the set of neighbors of node  $v \in V$  and  $\mathcal{R}_{(v,d)}^l$  is equal to the projected data,  $\mathbf{M}_{(i,:)}(\alpha) \cdot \mathbf{W}_{(:,d)}$  for the walk length  $l$ , and  $\mathcal{R}_{(v,d)}^0$  is initialized to 0.

Algorithm 1 provides the pseudocode of NodeSig. Firstly, we generate the projection matrix by sampling the weights from the Cauchy distribution with unit scale. The samples are further divided by  $\sum_{l=1}^L \alpha^l$ , because the row sums of  $\mathbf{M}(\alpha)$  must be equal to 1. Then, we compute the terms  $\mathcal{R}_{(v,d)}^l$  by propagating the weights in Line 9 at each walk iteration  $l < L$ . Note that, the term  $R$  in the pseudocode is a vector of length  $\mathcal{D}$ , thus we obtain the final representation of each node using the signs of  $\mathcal{R}_{(v,d)}^L$ .

### 3.3 Time and Space Complexity

As we can observe in Algorithm 1, the main cumbersome point of NodeSig is caused by the update rule defined in Eq. (1), which corresponds to Line 9 of the pseudocode. The update rule must be repeated  $|\mathcal{N}(v)|$  times for each node  $v \in V$ , thus it requires  $2 \cdot m \cdot \mathcal{D}$  multiplication operations at the walk step  $l$  ( $1 \leq l \leq L$ ) for a network consisting of  $m$  edges and for embedding vectors of dimension  $\mathcal{D}$ . Hence, the overall time complexity of the algorithm for a given projection matrix is  $\mathcal{O}(m \cdot L \cdot \mathcal{D})$ . During the running course of the algorithm, we need to keep the projection matrix  $\mathbf{W}$  in memory, and each node requires  $\mathcal{D}$  space for storing the  $\mathcal{R}_{(v,d)}^l$  values in the update rule of Eq. (1), thus we need  $\mathcal{O}(N \cdot \mathcal{D})$  space in total. Note that, the performance of the algorithm can be boosted by using parallel processing for each dimension of embedding vectors or for Line 6, since the required computation for each node is independent of each other.

### 3.4 Updating for Dynamic Networks

Many real-world networks change over time with the insertion of new edges or the removal of existing ones; thus, the embedding vectors should efficiently be updated instead of being recalculated from scratch. If an edge is added or removed for a pair of nodes  $(u, v) \in V \times V$ , the terms  $\mathcal{R}_{(w,:)}^l$  in Eq. (1) for node  $w \in V$  are affected, for all  $l > k := \min\{\text{dist}(w, u), \text{dist}(w, v)\}$ —thus, it suffices to update only these affected terms. The transition probabilities for nodes  $u$  and  $v$  also change even though the remaining nodes are not affected, so all the terms  $\mathbf{P}_{(v,:)}$  must be divided by  $\sum_{w \in \mathcal{N}(v)} P_{(v,w)}$  in order to normalize the transition probabilities and similarly the same procedure must be also applied for node  $u$  after each edge insertion and deletion operation.

## 4 PERFORMANCE EVALUATION

In this section, we report empirical evaluation results demonstrating the effectiveness and efficiency of NodeSig compared to baseline algorithms. All the experiments have been performed on an Intel Xeon 2.4GHz CPU server (32 Cores) with 60GB of memory.

---

### Algorithm 1: NodeSig

---

**Input:** Graph  $\mathcal{G} = (V, E)$  with the transition matrix  $\mathbf{P}$ ,  
 Embedding size  $\mathcal{D}$ , Walk length  $L$ , Importance factor  $\alpha$   
**Output:** Embedding vectors  $E[v] \in \mathbb{R}^{\mathcal{D}}$  for each node  $v \in V$

```

1 for each node  $v \in V$  do
2    $\mathcal{R}[v] \leftarrow \mathbf{0}_{\mathcal{D}} = (0, \dots, 0)$ ;
3    $W[v] \sim \text{Cauchy}(0, 1)^{\mathcal{D}} / \sum_{l=1}^L \alpha^l$ ;
4 end
5 for  $l \leftarrow 1$  to  $L$  do
6   for each node  $v \in V$  do
7      $\text{temp}[v] \leftarrow \mathbf{0}_{\mathcal{D}} = (0, \dots, 0)$ ;
8     for each neighbour node  $u \in \mathcal{N}(v)$  do
9        $\text{temp}[v] \leftarrow \text{temp}[v] + (W[u] + \mathcal{R}[u]) \times P[u, v]$ ;
10    end
11   end
12   for each node  $v \in V$  do
13      $\mathcal{R}[v] \leftarrow \alpha \times \text{temp}[v]$ ;
14   end
15 end
16 for each node  $v \in V$  do
17    $E[v] \leftarrow \text{sign}(\mathcal{R}[v])$ ;
18 end

```

---

### 4.1 Datasets and Baseline Models

**Datasets.** We perform experiments on networks of different scales and type. (i) *Blogcatalog* [27] is a social network constructed by using the relationships among bloggers, where node labels indicate the blog categories specified by the blogger. (ii) *Cora* [25] is a citation network in which nodes corresponds to articles, while labels indicate document categories. (iii) *DBLP* [21] is a co-authorship network, in which an edge between authors indicates co-authorship relationship, while node labels represent research areas. (iv) *PPI* [19] is a protein-protein interaction subgraph for Homo Sapiens. (v) *Youtube* [28], the largest network in our experiments, has been crawled from the corresponding video sharing platform. Node labels indicate categories of videos. All the networks used in the empirical analysis are unweighted and undirected (the direction of edges are discarded), in order to be consistent in the evaluation. The characteristics of the datasets are reported in Table 1.

**Baseline models.** We have considered six representative baseline methods in the experimental evaluation. In particular, the first two of these methods correspond to widely used node embedding models, while the remaining ones constitute more recent models aiming to address the scalability challenge. For all methods, we learn embedding vectors of size 128.

- Node2Vec [8] is a biased random walk strategy based on the SkipGram [15] model. Parameters  $p$  and  $q$  which control the behavior of the random walk are simply set to 1.0.
- HOPE [18] is a matrix factorization-based method aiming to capture high-order proximity among nodes. Parameter  $\beta$  is set to the default value  $0.5/r$ , where  $r$  is the spectral radius of the adjacency matrix.

Networks	<i>Blogcatalog</i>	<i>Cora</i>	<i>DBLP</i>	<i>PPI</i>	<i>Youtube</i>
# Nodes	10,312	2,708	27,199	3,890	1,138,499
# Edges	333,983	5,278	66,832	38,739	2,990,443
# Labels	39	7	4	50	47
# Density	$6.3 \times 10^{-3}$	$1.4 \times 10^{-3}$	$1.8 \times 10^{-4}$	$5.1 \times 10^{-3}$	$4.6 \times 10^{-6}$

Table 1: Characteristics of networks.

- NETSMF [22] is a sparse matrix factorization method, recently proposed to deal with the scalability constraints of NETMF [23] – a model that relies on the pointwise mutual information of node co-occurrences. In our experiments, we set the rank parameter to 512 and the number of rounds to 10,000 for all networks except *PPI* and *Youtube* in which the model was unable to run. In these cases, the rank parameter is set to 256, while the number of rounds to 1,000 and 50 for *PPI* and *Youtube*, respectively.
- RANDNE [38] is a highly efficient embedding method based on Gaussian random projections, and one of the most widely applied scalable models. The experiments were conducted by setting the parameters suggested by the authors. In the case of node classification, the transition matrix with parameter values  $q = 3$  and  $weights = [1, 10^2, 10^4, 10^5]$  was used, while the adjacency matrix with  $q = 2$  and  $weights = [1, 1, 10^{-2}]$  was considered in the link prediction experiments.
- LOUVAINNE [1] constructs a hierarchical subgraph structure and aggregates the node representations learned at each different level to obtain the final embeddings. In our experiments, we have used the default parameter settings and  $\alpha$  was set to 0.01.
- NODESKETCH [34] learns embeddings in the *Hamming* space, using MINHASH signatures. We have used the best-performing settings recommended by the authors, and the values of  $\alpha$  and order  $k$  are set to 0.1 and 20 respectively for *Cora*.

For the proposed NODESIG model, we set the importance factor  $\alpha$  to 1 in all the experiments. The walk length is set to 3 for *Cora* and *Blogcatalog*, and to 5 for all the other networks in the classification experiment. For the link prediction task, the walk length is chosen as 15 for all networks. We set the dimension size of the embedding vectors to 8,196 bits in order to be consistent with the experiments with the baseline methods, since modern computer architectures use 8 Bytes for storing floating point data types.

## 4.2 Multi-label Node Classification

The networks described previously consist of nodes having at least one or more labels. In the classification task, our goal is to correctly infer the labels of nodes chosen for the testing set, using the learned representations and the labels of nodes in the rest of the network, namely the nodes in the training set. The evaluation follows a strategy similar to the one used by baseline models [34].

**4.2.1 Experimental set-up.** The experiments are carried out by training an one-vs-rest SVM classifier with a pre-computed kernel, which is designed by computing the similarities of node embeddings. The similarity measure is chosen depending on the algorithm that we use to learn representations. More specifically, the *Hamming*

similarity for NODESKETCH and the *Cosine* similarity for the rest baselines methods are chosen in order to build the kernels for the classifier. For NODESIG, we use the *chi* similarity  $\chi$ , defined as  $1 - \sqrt{d_{\chi^2}}$ , where  $d_{\chi^2}$  is equal to

$$d_{\chi^2} := \sum_{i=1}^{\mathcal{D}} \frac{(\mathbf{x}_i - \mathbf{y}_i)^2}{\mathbf{x}_i + \mathbf{y}_i} = \sum_{i=1}^{\mathcal{D}} (\mathbf{x}_i + \mathbf{y}_i) - \sum_{i=1}^{\mathcal{D}} \frac{4\mathbf{x}_i\mathbf{y}_i}{\mathbf{x}_i + \mathbf{y}_i} = 2 - 2\rho_{\chi^2},$$

for the vectors satisfying  $\sum_i \mathbf{x}_i = \sum_i \mathbf{y}_i = 1$  and  $\mathbf{x}_i \geq 0, \mathbf{y}_i \geq 0$  for all  $1 \leq i \leq \mathcal{D}$ .

**4.2.2 Experimental results.** For the multi-label node classification task, Tables 2-6 report the average Micro- $F_1$  and Macro- $F_1$  scores over 10 runs, where the experiments are performed on different training set sizes. The symbol "-" is used to indicate that the corresponding algorithm is unable to run due to excessive memory usage or because it requires more than one day to complete. The best and second best performing models for each training ratio (10%, 50%, and 90%) are indicated with bold and underlined text, respectively.

	Micro- $F_1$			Macro- $F_1$		
	10%	50%	90%	10%	50%	90%
HOPE	0.305	0.316	0.318	0.117	0.118	0.123
NODE2VEC	0.341	0.348	0.348	0.158	0.161	0.164
NETSMF	<b>0.374</b>	<u>0.399</u>	<u>0.397</u>	<b>0.200</b>	0.221	0.207
LOUVAINNE	0.044	0.149	0.150	0.020	0.037	0.038
RANDNE	0.322	0.342	0.347	0.147	0.170	0.171
NODESKETCH	0.305	0.381	0.395	0.147	<u>0.236</u>	<u>0.256</u>
NODESIG	<u>0.363</u>	<b>0.409</b>	<b>0.421</b>	<u>0.197</u>	<b>0.266</b>	<b>0.291</b>

Table 2: Micro- $F_1$  and Macro- $F_1$  classification scores for varying training set ratios of the *Blogcatalog* network.

	Micro- $F_1$			Macro- $F_1$		
	10%	50%	90%	10%	50%	90%
HOPE	0.694	0.781	0.800	0.678	0.775	0.795
NODE2VEC	<b>0.765</b>	0.808	0.816	<u>0.751</u>	0.796	0.800
NETSMF	<u>0.763</u>	0.828	0.840	<b>0.754</b>	0.818	0.830
LOUVAINNE	0.693	0.711	0.718	0.667	0.680	0.681
RANDNE	0.580	0.674	0.697	0.558	0.667	0.689
NODESKETCH	0.727	<u>0.844</u>	<u>0.880</u>	0.707	<u>0.837</u>	<u>0.871</u>
NODESIG	0.750	<b>0.846</b>	<b>0.893</b>	0.736	<b>0.838</b>	<b>0.886</b>

Table 3: Micro- $F_1$  and Macro- $F_1$  classification scores for varying training set ratios of the *Cora* network.

As we observe, NODESIG consistently outperforms the baselines for higher training ratios on the *Blogcatalog* and *Cora* networks, while the obtained Macro- $F_1$  score is very close to the performance of NETSMF for 10% training ratio on *Blogcatalog*. In the case of the *Cora* network which corresponds to the smallest one used in our study, NODE2VEC shows better performance for small training ratio of 10%. For the *Youtube* and *DBLP* networks, the proposed NODESIG model along with *NodeSketch* perform equally well. This

	Micro- $F_1$			Macro- $F_1$		
	10%	50%	90%	10%	50%	90%
HOPE	0.621	0.632	0.634	0.532	0.540	0.545
Node2Vec	0.622	0.633	0.633	0.513	0.539	0.538
NETSMF	0.627	0.648	0.650	0.530	0.578	0.580
LOUVAINNE	0.502	0.502	0.494	0.367	0.358	0.325
RANDNE	0.413	0.438	0.438	0.223	0.256	0.254
NodeSketch	<u>0.656</u>	<b>0.845</b>	<b>0.906</b>	<u>0.601</u>	<b>0.829</b>	<b>0.894</b>
NodeSig	<b>0.705</b>	<b>0.845</b>	<u>0.893</u>	<b>0.661</b>	<u>0.826</u>	<u>0.879</u>

**Table 4: Micro- $F_1$  and Macro- $F_1$  classification scores for varying training set ratios of the DBLP network.**

	Micro- $F_1$			Macro- $F_1$		
	10%	50%	90%	10%	50%	90%
HOPE	0.131	0.151	0.146	0.082	0.085	0.078
Node2Vec	0.140	0.160	0.141	0.084	0.088	0.072
NETSMF	0.153	0.173	0.169	0.099	0.106	0.105
LOUVAINNE	0.044	0.052	0.055	0.025	0.023	0.020
RANDNE	0.136	0.160	0.142	0.082	0.091	0.077
NodeSketch	<u>0.146</u>	<u>0.226</u>	<u>0.247</u>	<u>0.096</u>	<u>0.183</u>	<b>0.204</b>
NodeSig	<b>0.180</b>	<b>0.236</b>	<b>0.253</b>	<b>0.121</b>	<b>0.186</b>	<u>0.197</u>

**Table 5: Micro- $F_1$  and Macro- $F_1$  classification scores for varying training set ratios of the PPI network.**

	Micro- $F_1$			Macro- $F_1$		
	10%	50%	90%	10%	50%	90%
HOPE	0.342	0.343	0.342	0.198	0.203	0.206
Node2Vec	-	-	-	-	-	-
NETSMF	0.380	0.370	0.360	0.259	0.249	0.229
LOUVAINNE	0.248	0.252	0.243	0.060	0.065	0.064
RANDNE	0.331	0.340	0.341	0.201	0.217	0.216
NodeSketch	0.439	<b>0.467</b>	<b>0.474</b>	0.364	<b>0.412</b>	<b>0.427</b>
NodeSig	<b>0.455</b>	<u>0.464</u>	<u>0.464</u>	<b>0.387</b>	<u>0.407</u>	<u>0.405</u>

**Table 6: Micro- $F_1$  and Macro- $F_1$  classification scores for varying training set ratios of the Youtube network.**

is quite surprising, since both these methods that correspond to data-independent hashing techniques offer a clear performance gain over traditional models, such as Node2Vec and HOPE. Lastly, for the PPI dataset, NodeSig obtains consistently the highest scores for Micro- $F_1$ , while its main competitor NodeSketch has close performance for the Macro- $F_1$  score.

### 4.3 Link Prediction

The second downstream task used to assess the quality of node embeddings is the one of link prediction.

**4.3.1 Experimental set-up.** Half of the edges of a given network are removed by still keeping the residual network connected. Node embeddings are learned on the rest of the graph. The removed edges are considered as positive samples for the testing set, while the same number of node pairs which does not exist in the initial network is separately sampled for training and testing sets in order

to form the negative samples. As it has been described in Section 4.2, we build the features corresponding to the node pair samples using the similarities between embedding vectors; the similarity measure is chosen depending on the algorithm that we use to extract the representations. Since the Youtube dataset is relatively larger than the rest networks, we work on 7% of its initial size. We use the logistic regression classifier for training, and we provide the Area Under Curve (AUC) scores in Table 7.

**4.3.2 Experimental results.** For the link prediction task, NodeSig acquires the highest AUC scores on three datasets, while it is also the second best performing model for the remaining two. In the case of the Youtube dataset, all baselines demonstrate comparable results. Although Node2Vec shows good performance across most datasets in the link prediction task, it does not perform well on the Blogcatalog networks, mainly because its high density. On the other hand, NodeSig reaches the highest score on this dataset, with a clear difference to its main competitor, NodeSketch.

	Blogcatalog	Cora	Dblp	PPI	Youtube
HOPE	0.5169	0.6617	0.7687	0.5241	0.5143
Node2Vec	0.5954	<b>0.7467</b>	<u>0.8443</u>	<u>0.6152</u>	0.5307
NETSMF	0.5699	0.7171	0.8320	0.5488	<b>0.5409</b>
LOUVAINNE	0.5007	0.6977	0.7852	0.5748	0.5292
RANDNE	0.6215	0.5901	0.6972	0.5039	0.5112
NodeSketch	<u>0.7034</u>	0.7097	0.7140	0.5117	0.5103
NodeSig	<b>0.8223</b>	<u>0.7400</u>	<b>0.8596</b>	<b>0.6553</b>	<u>0.5361</u>

**Table 7: Area Under Curve (AUC) scores for link prediction.**

### 4.4 Parameter Sensitivity

Next, we analyze how the behavior of the proposed NodeSig algorithm is affected by the parameter setting. More specifically, we concentrate on the influence of three parameters, namely walk length  $L$ , importance factor  $\alpha$  and dimension size  $\mathcal{D}$ , examining the impact on the Cora network.

**4.4.1 Effect of walk length.** In order to examine the influence of the walk length on the performance, we perform experiments for varying lengths by fixing the importance factor  $\alpha$  to 1.0. Figure 3a depicts the Micro- $F_1$  scores for different training ratios. We observe a significant increase in performance when the walk length increases, particularly for small training ratios and walk lengths. Although it shows a wavy behavior for the largest training ratio, there is a logarithmic improvement depending on the walk length. NodeSig better captures the structural properties of the network in longer walks, thus the low performance observed on small training ratios can be compensated with longer walks.

**4.4.2 Effect of importance factor.** The importance factor is another parameter of NodeSig, which controls the impact of walks of different lengths: the importance of the higher levels is increasing for  $\alpha > 1$ , while it can be diminished choosing  $\alpha < 1$ . Figure 3b depicts the performance of NodeSig on the Cora network, fixing the walk length value to 5. Although we do not observe a steady behavior for the large training set, higher values of  $\alpha$ , especially around 4, positively contribute to the performance; values smaller than 1 have negative impact on the performance.



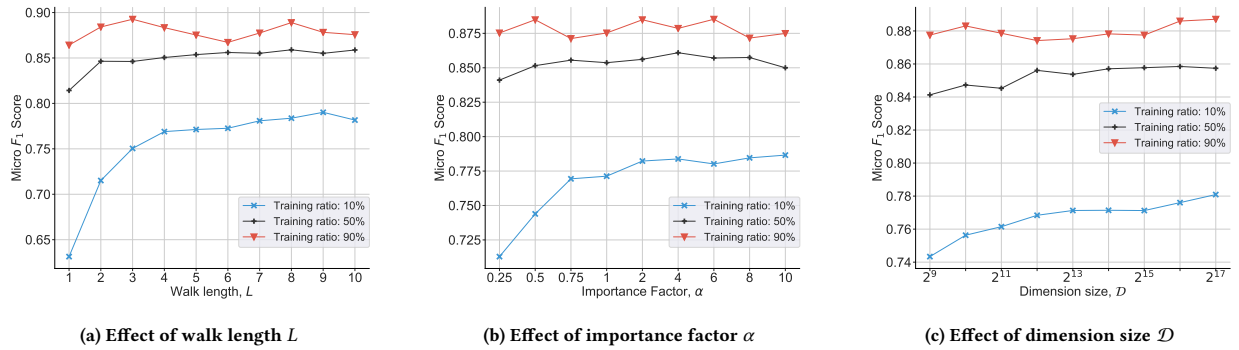


Figure 3: Influence of various parameters on the Micro- $F_1$  score on the Cora network for varying training set ratios.

**4.4.3 Effect of dimension size.** The dimension size is a crucial parameter affecting the performance of the algorithm, since a better approximation to the  $\chi^2$  similarity measure can be obtained for larger dimension sizes, following *Hoeffding's* inequality [10]. Therefore, we perform experiments for varying dimension sizes, by fixing the walk length to 5. Figure 3c depicts the Micro- $F_1$  scores of the classification experiment for different dimension sizes ranging from  $2^9$  to  $2^{17}$ . Although we have fluctuating scores on the large training set due to the randomized behavior of the approach, the impact of the dimension size can be observed clearly on the small training set size. On the other hand, we observe an almost stable behavior for the training ratio of 50%, encouraging the use of small embedding sizes towards reducing storage requirements.

## 4.5 Running Time Comparison

The running time is of great importance, since the embedding models are expected to scale and run in reasonable time on large graphs. We have recorded the elapsed real (wall clock) time of all baseline models including the one of NODESIG, and the results are provided in Table 8. The *Random* network indicates the  $\mathcal{G}_{n,p}$  Erdős-Renyi random graph model, using  $n = 100,000$  and  $p = 0.0001$ . All the experiments have been conducted on the server whose specifications have been given in the beginning of Section 4. We use 32 threads for each algorithm, when it is applicable. If a model cannot run due to excessive memory usage with the parameter settings described in Section 4.1, the parameters are set to values closest to its default parameters, which enables the models to run in reasonable time. For NODESIG, the walk length is set to 5, and  $\alpha$  to 1 in all experiments.

As we observe, NODESIG runs faster than HOPE, NODE2VEC as well as NETSMF. This is happening because HOPE requires an expensive matrix factorization, while NODE2VEC needs to simulate random walks to obtain their exact realizations. Although NETSMF has been proposed as the scalable extension of another matrix factorization model [23], we have observed that it requires high memory footprint; therefore, we could not run it with the default parameters specified by the authors of the corresponding paper. Furthermore, although the remaining baseline methods run faster compared to NODESIG, as we have already presented, the proposed model generally outperforms them both in classification and link prediction tasks. These experiments further support the intuition

about designing NODESIG, as an expressive model that balances accuracy and running time.

	<i>Blogcatalog</i>	<i>Cora</i>	<i>DBLP</i>	<i>PP1</i>	<i>Youtube</i>	<i>Random</i>	<i>Speedup</i>
HOPE	89	26	185	32	9183	1117	1.8x
NODE2VEC	1187	15	164	62	-	749	5.6x
NETSMF	2241	15	183	13	5399	454	1.4x
LOUVAINNE	0.29	0.06	0.21	0.13	5.70	1.2	0.001x
RANDNE	3.18	1.50	6.22	2.02	161.8	23	0.03x
NODESKETCH	106.84	13.46	21.93	9.26	2300	190	0.45x
NODESIG	120	4.38	41	14	5508	209	1.0x

Table 8: Running time (in seconds) and average speedup.

## 5 CONCLUSIONS AND FUTURE WORK

In this paper, we have introduced NODESIG, an efficient binary node embedding model. Each component of model has properly been designed to improve scalability without sacrificing effectiveness on downstream tasks. NODESIG exploits random walk diffusion probabilities via stable random projection hashing, towards efficiently computing representations in the Hamming space that approximate the chi-square similarity. The experimental results have demonstrated that NODESIG outperformed in accuracy recent highly-scalable models, being able to run within reasonable time duration, while at the same time it shows comparable or even better accuracy with respect to widely used baseline methods in multi-label node classification and link prediction. As future work, we plan to further study the properties of the model for attributed and dynamic networks.

## REFERENCES

- [1] Ayan Kumar Bhowmick, Koushik Meneni, Maximilien Danisch, Jean-Loup Guillaume, and Bivas Mitra. Louvainne: Hierarchical louvain method for high quality and scalable network embedding. In *WSDM*, pages 43–51, 2020.
- [2] A. Broder. On the resemblance and containment of documents. In *Proceedings of the Compression and Complexity of Sequences 1997*, page 21, 1997.
- [3] Shaosheng Cao, Wei Lu, and Qionghai Xu. GraRep: Learning graph representations with global structural information. In *CIKM*, pages 891–900, 2015.
- [4] Abdulkadir Çelikkanat and Fragkiskos D. Malliaros. Exponential family graph embeddings. In *AAAI*, pages 3357–3364, 2020.



- [5] Haochen Chen, Bryan Perozzi, Yifan Hu, and Steven Skiena. HARP: hierarchical representation learning for networks. In *AAAI*, pages 2127–2134, 2018.
- [6] Haochen Chen, Syed Fahad Sultan, Yingtao Tian, Muhao Chen, and Steven Skiena. Fast and accurate network embeddings via very sparse random projection. In *CIKM*, pages 399–408, 2019.
- [7] Michel X. Goemans and David P. Williamson. Improved approximation algorithms for maximum cut and satisfiability problems using semidefinite programming. *J. ACM*, 42, 1995.
- [8] Aditya Grover and Jure Leskovec. Node2vec: Scalable feature learning for networks. In *KDD*, pages 855–864, 2016.
- [9] William L. Hamilton, Rex Ying, and Jure Leskovec. Representation learning on graphs: Methods and applications. *IEEE Data Eng. Bull.*, 40:52–74, 2017.
- [10] Wassily Hoeffding. Probability inequalities for sums of bounded random variables. *Journal of the American Statistical Association*, 58:13–30, 1963.
- [11] V. T. L. Huong, D. Park, D. Woo, and Yunsik Lee. Centroid neural network with chi square distance measure for texture classification. In *IJCNN*, pages 1310–1315, 2009.
- [12] William B. Johnson, Joram Lindenstrauss, and Gideon Schechtman. Extensions of lipschitz maps into banach spaces. *Israel Journal of Mathematics*, 54:129–138, 1986.
- [13] Ping Li, Gennady Samorodnitsky, and John Hopcroft. Sign cauchy projections and chi-square kernel. In *NIPS*, 2013.
- [14] Defu Lian, Kai Zheng, Vincent W. Zheng, Yong Ge, Longbing Cao, Ivor W. Tsang, and Xing Xie. High-order proximity preserving information network hashing. In *KDD*, pages 1744–1753, 2018.
- [15] Tomas Mikolov, Ilya Sutskever, Kai Chen, Greg Corrado, and Jeffrey Dean. Distributed representations of words and phrases and their compositionality. In *NIPS*, pages 3111–3119, 2013.
- [16] M.E.J. Newman. The structure and function of complex networks. *SIAM review*, 45(2):167–256, 2003.
- [17] Duong Nguyen and Fragkiskos D. Malliaros. BiasedWalk: Biased sampling for representation learning on graphs. In *Big Data*, pages 4045–4053, 2018.
- [18] Mingdong Ou, Peng Cui, Jian Pei, Ziwei Zhang, and Wenwu Zhu. Asymmetric transitivity preserving graph embedding. In *KDD*, pages 1105–1114, 2016.
- [19] Rose Oughtred, Chris Stark, Bobby-Joe Breitkreutz, Jennifer Rust, Lorrie Boucher, Christie Chang, Nadine Kolas, Lara O'Donnell, Genie Leung, Rochelle McAdam, Frederick Zhang, Sonam Dolma, Andrew Willems, Jasmin Coulombe-Huntington, Andrew Chatr-aryamontri, Kara Dolinski, and Mike Tyers. The BioGRID interaction database: 2019 update. *Nucleic Acids Research*, 47:D529–D541, 2018.
- [20] Bryan Perozzi, Rami Al-Rfou, and Steven Skiena. Deepwalk: Online learning of social representations. In *KDD*, pages 701–710, 2014.
- [21] Bryan Perozzi, Vivek Kulkarni, Haochen Chen, and Steven Skiena. Don't walk, skip! online learning of multi-scale network embeddings. In *ASONAM*, pages 258–265, 2017.
- [22] Jiezhong Qiu, Yuxiao Dong, Hao Ma, Jian Li, Chi Wang, Kuansan Wang, and Jie Tang. NetSMF: Large-scale network embedding as sparse matrix factorization. In *WWW*, pages 1509–1520, 2019.
- [23] Jiezhong Qiu, Yuxiao Dong, Hao Ma, Jian Li, Kuansan Wang, and Jie Tang. Network embedding as matrix factorization: Unifying deepwalk, line, pte, and node2vec. In *WSDM*, pages 459–467, 2018.
- [24] Sam T. Roweis and Lawrence K. Saul. Nonlinear Dimensionality Reduction by Locally Linear Embedding. *Science*, 290:2323–2326, 2000.
- [25] Prithviraj Sen, Galileo Namata, Mustafa Bilgic, Lise Getoor, Brian Gallagher, and Tina Eliassi-Rad. Collective classification in network data. *AI magazine*, 2008.
- [26] Jian Tang, Meng Qu, Mingzhe Wang, Ming Zhang, Jun Yan, and Qiaozhu Mei. LINE: Large-scale information network embedding. In *WWW*, pages 1067–1077, 2015.
- [27] Lei Tang and Huan Liu. Relational learning via latent social dimensions. In *KDD*, pages 817–826, 2009.
- [28] Lei Tang and Huan Liu. Scalable learning of collective behavior based on sparse social dimensions. In *CIKM*, 2009.
- [29] Joshua B. Tenenbaum, Vin de Silva, and John C. Langford. A global geometric framework for nonlinear dimensionality reduction. *Science*, 290:2319, 2000.
- [30] Santosh Vempala. *The random projection method*. American Mathematical Soc., 2001.
- [31] Daixin Wang, Peng Cui, and Wenwu Zhu. Structural deep network embedding. In *KDD*, pages 1225–1234, 2016.
- [32] Jingdong Wang, Ting Zhang, Jingkuan Song, Nicu Sebe, and Heng Tao Shen. A survey on learning to hash. *IEEE Trans. Pattern Anal. Mach. Intell.*, 40(4):769–790, 2018.
- [33] Wei Wu, Bin Li, Ling Chen, and Chengqi Zhang. Efficient attributed network embedding via recursive randomized hashing. In *IJCAI*, pages 2861–2867, 2018.
- [34] Dingqi Yang, Paolo Rosso, Bin Li, and Philippe Cudre-Mauroux. Nodsketch: Highly-efficient graph embeddings via recursive sketching. In *KDD*, pages 1162–1172, 2019.
- [35] Chen Ye, Jian Wu, Victor S. Sheng, Shiquan Zhao, Pengpeng Zhao, and Zhiming Cui. Multi-label active learning with chi-square statistics for image classification. In *ICMR*, 2015.
- [36] Xinyang Yi, Constantine Caramanis, and Eric Price. Binary embedding: Fundamental limits and fast algorithm. In *ICML*, pages 2162–2170, 2015.
- [37] G. Young and A. S. Householder. Discussion of a set of points in terms of their mutual distances. *Psychometrika*, 3:19–22, 1938.
- [38] Z. Zhang, P. Cui, H. Li, X. Wang, and W. Zhu. Billion-scale network embedding with iterative random projection. In *ICDM*, pages 787–796, 2018.